Identification of ASYNAPTIC4, a Component of the Meiotic Chromosome Axis

Chambon, Aurélie; West, Allan; Vezon, Daniel; Horlow, Christine; De Muyt, Arnaud; Chelysheva, Liudmila; Ronceret, Arnaud; Darbyshire, Alice; Osman, Kim; Heckmann, Stefan; Franklin, F Chris H; Grelon, Mathilde

DOI:
10.1104/pp.17.01725

Short Title: ASY4, a new meiotic chromosome axis component

Corresponding author: Mathilde Grelon

Identification of a new component of the meiotic chromosome axis in *Arabidopsis thaliana*

Aurélie Chambon[1], Allan West[2], Daniel Vezon[1], Christine Horlow[1], Arnaud De Muyt[1], Liudmila Chelysheva[1], Arnaud Ronceret[1], Alice Darbyshire[2], Kim Osman[2], Stefan Heckmann[2], F. Chris. H. Franklin[2], Mathilde Grelon[1]

[1]Institut Jean-Pierre Bourgin, INRA, AgroParisTech, CNRS, Université Paris-Saclay, RD10, 78026 Versailles Cedex, France

[2]School of Biosciences, University of Birmingham, Edgbaston, Birmingham, United Kingdom

Abstract:

During the leptotene stage of prophase I of meiosis chromatids become organized into a linear looped array by a protein axis that forms along the loop bases. Establishment of the axis is essential for the subsequent synapsis of the homologous chromosome pairs and the progression of recombination to form genetic crossovers. Here we describe ASY4 a new component of the meiotic protein axis in *Arabidopsis thaliana*. ASY4 is a small coil-coiled protein that exhibits limited homology with the C-terminal region of the axis protein ASY3. We show using an eYFP-tagged ASY4 that the protein localizes to the chromosome axis throughout prophase I. Bi-molecular fluorescence reveals that ASY4 interacts with ASY1 and ASY3 and yeast two-hybrid analysis confirms a direct interaction between ASY4 and ASY3. Mutants lacking full-length ASY4 exhibit defective axis formation and are unable to complete synapsis. Although initiation of recombination appears unaffected in an *asy4* mutant, crossovers are significantly reduced and tend to group in the distal parts of the chromosomes. In summary, we have identified a new component of the meiotic chromosome axis that is required for normal axis formation and controlled crossover formation.

Introduction

Meiosis is the specialised cell division that generates the haploid cells from which the gametes will be generated. In most organisms this ploidy reduction is achieved by segregating, first, the homologous chromosomes from each other (meiosis I), then, by separating the sister chromatids at meiosis II. The correct meiotic course relies on a series of coordinated mechanisms that take place during meiotic prophase I. They include the organisation of sister chromatids along a common proteinaceous axis (the axial element, AE), the pairing and the synapsis of these axes, recombination and the formation of at least one crossover (CO) per homologous pair (Zickler and Kleckner, 1999).

The AEs are assembled early during meiotic prophase I, defining the leptotene stage. Then, axes from the homologous chromosomes become connected by the polymerisation of the central element of the synaptonemal complex (SC), forming the lateral elements (LEs) of the SC. The polymerisation of the SC is complete by pachytene, a stage at which the maturation of recombination intermediates into COs is achieved, at least in *S. cerevisiae* (Zickler and Kleckner, 1999). Next, the central element of the SC is disassembled while the chromosome axis participates in the dramatic chromosome condensation that occurs during the remaining steps of meiotic prophase I (diplotene, diakinesis).

Therefore, a defining feature of meiotic chromosomes is that sister chromatids share a chromosome axis to which they are anchored, forming regular arrays of chromatin loops. Because most of the recombination proteins are axis-associated, it has been proposed that meiotic chromosome axes form a scaffold on which meiotic recombination takes place (Blat et al., 2002; Panizza et al., 2011). Notwithstanding these structural roles, chromosome axes also appear highly flexible and dynamic. Their physical association with the chromosomes depends on and is responsive to underlying transcriptional activity (Sun et al., 2015). Some of their components are displaced upon synapsis and during recombination, where there is a requirement for localized axis exchange at CO sites.

Chromosome axes are composed of various protein families (Zickler and Kleckner, 1999). Cohesins (and notably the meiosis-specific Rec8 protein) as well as cohesin-associated factors such as the condensins are key components of the AEs. Cohesins form ring-shaped complexes that associate sister chromatids together after replication and that in *S. cerevisiae* anchor the other axial element proteins to chromatin (Sun et al., 2015). The HORMA domain proteins (Hop1 in *S. cerevisiae*, HormaD1 and HormaD2 in mammals, ASY1/PAIR2 in plants, HIM-3, HTP-1, HTP-2, and HTP-3 in *C. elegans*) also represent major components of the meiotic chromosomal axes that in *C. elegans* constitute the linker between the cohesins and the SC central element (Pattabiraman et al., 2017). In several organisms, including *A. thaliana*, their axis association is negatively regulated by synapsis (Börner et al., 2008; Wojtasz et al., 2009; Lambing et al., 2015). The last class of known axial element proteins contains the *S. cerevisiae* Red1, the mouse SYCP2 and SYCP3 (SCP2 and SCP3 in rat), and the plant ASY3/PAIR3/DSY2 (Wang et al., 2011; Ferdous et al., 2012; Lee et al., 2015). All these proteins are meiosis-specific components of the axial element. Red1, SYCP2/SCP2 and ASY3/PAIR3 are large proteins that show limited sequence similarities, suggesting that they could be distantly related (Offenberg et al., 1998; Ferdous et al., 2012). Concerning the mammalian SYCP3/SCP3, they are small proteins that show sequence similarities with SYCP2/SCP2 with which they interact through their coiled-coil regions. They are thought to represent key structural components of the mammalian meiotic chromosome axes since notably, they form multi-stranded fibres that mimic the AEs when ectopically expressed in somatic cells (Yuan et al., 1998; Pelttari et al., 2001). In addition, structural resolution of the human SYCP3 protein revealed that it forms elongated helical tetrameric structures that self-assemble into AE-like fibres that possess the intrinsic capacity of mediating dsDNA compaction (Syrjänen et al., 2014; Syrjänen et al., 2017).

Mutants defective in any component of the AE exhibit substantial perturbation of the meiotic recombination process. The plant HORMA domain-containing protein ASY1 is not required for normal DSB formation but for DMC1 stabilisation on recombination sites (Armstrong et al., 2002; Sanchez-Moran et al., 2007). In consequence, in *asy1* mutants, meiotic DSBs are predominantly repaired using a sister chromatid as template, as is the case in a *dmc1* mutant, provoking a shortage in CO formation

(Sanchez-Moran et al., 2007). The axial protein ASY3/PAIR3/DSY2, on the other hand, is required for normal levels of DSB formation in *A. thaliana* and in maize (Ferdous et al., 2012; Lee et al., 2015). It is also required for normal ASY1 assembly onto the chromosome axis, and it interacts with ASY1 (Ferdous et al., 2012; Lee et al., 2015) and with ZYP1 (Lee et al., 2015).

In this manuscript, we present the identification of ASY4, a short coiled-coil containing protein showing similarity with the ASY3 C-terminus coiled coil region. We show that ASY4 is an axis-associated protein that interacts with ASY1 and ASY3. We also found that ASY4 is required for normal ASY1 and ASY3 localisation, for full synapsis and for CO formation.

120

Results

Identification of *ASY4*, a meiotic gene with similarity to *ASY3*

A BlastP search against the *A. thaliana* genome using the ASY3 protein (At2G46980) as a query identified the uncharacterised At2g33793 protein (hereafter called ASY4) as showing 29% identity and 45% similarity with 142 aa of the C-terminus region of ASY3 (Figure 1). While ASY3 is a large protein (793 aa, 88 kD), ASY4 is only 212 aa long (25kD). Its sequence does not contain any known functional domains and most of the ASY4 protein is predicted to form coiled-coils (aa 71-183, Figure 1). ASY4 homologous proteins can be identified in *Tracheophyta* sequenced genomes (that include flowering plant genomes and *Sellaginella moellendorffii*). Outside *Tracheophyta,* ASY4 homologous sequence is found in *Marchantia polymorpha* but not in mosses. RT-PCR on cDNAs isolated from different organs from wild-type plants showed that *ASY4* is expressed predominantly in flower buds (SupData_1).

To analyse *ASY4* function, we characterised two independent mutant lines in At2g33793. One was available in the public databases: line SK22114 (Stock: CS1006148, later referred to as *asy4-1*). The second one (*asy4-2*) was isolated by PCR-screening of MPIPZ (Cologne) *A. thaliana* T-DNA insertion mutants (Ríos et al., 2002). Insertions in *asy4-1* and *asy4-2* are located in *ASY4* fourth and fifth exons, respectively and are associated with deletions of 17 and 19 bp respectively (Figure 1 and SupData_2). Residual transcription corresponding to the 5' end of the gene can be detected in both mutants (SupData_1). They could potentially generate a C-terminally truncated protein of 92 or 106 aa respectively.

Both *asy4* mutants investigated in this study showed normal vegetative growth (not shown) but fertility defects (SupData_3) that correlated with meiotic defects (Figure 2). During prophase I in wild-type meiosis the ten *A. thaliana* chromosomes condense and recombine resulting in the formation of five bivalents, each consisting of two homologous chromosomes attached to each other by sister chromatid cohesion and chiasmata (the cytological manifestation of COs), which become visible at diakinesis. Synapsis (the close association of two chromosomes mediated by the SC) begins at zygotene and is complete by pachytene. At metaphase I, the five

Figure 1

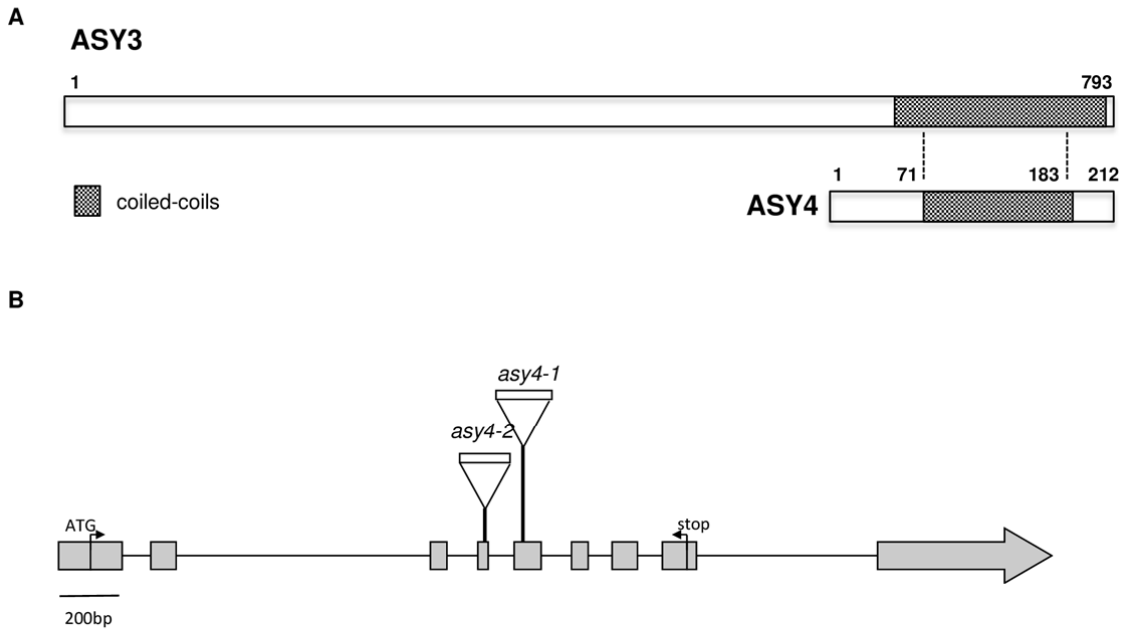

Figure 1:: Schematic representation of ASY4 protein and gene.
A. The ASY4 protein shows similarities with ASY3 C-terminal region (dashed lines). Predicted coiled-coils of both proteins are indicated by grey boxes.
B. *ASY4* open reading frame and position of the T-DNA insertion in *asy4-1* and *asy4-2* mutants. Exons are shown as grey boxes.

bivalents are easily distinguishable aligned on the metaphase plate. During anaphase I, each chromosome separates from its homologue, leading to the formation of dyads corresponding to two pools of five chromosomes. The second meiotic division then separates the sister chromatids, generating four pools of five chromosomes, which gives rise to tetrads of four haploid daughter cells. In *asy4* mutants, each of these meiotic stages can be identified, although full synapsis was not detected. Moreover, the presence of univalent chromosomes at diakinesis and unbalanced tetrads (illustrated for *asy4-1* in Figure 2) indicates a defect in CO formation.

The reduction in chiasma number observed in *asy4* meiocytes was quantified at the transition between metaphase I and anaphase I by estimating the number of chiasma based on bivalent shape. Rod bivalents reflect the occurrence of a minimum of one

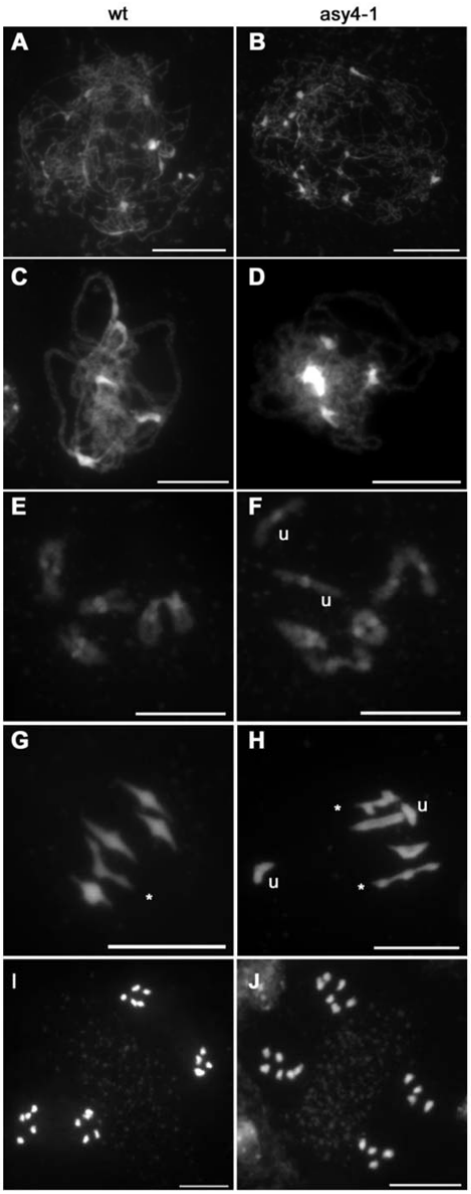

Figure 2:ASY4 is required for normal meiosis.
(A-J) DAPI staining of meiotic chromosomes in wild type (A,C,E,G,I) and *asy4-1* (B,D,F,H,J). (A,B) Leptotene; (C) Pachytene; (D) Partial synapsis typical of the defects of synapsis observed in *asy4* mutants; (E,F) Diakinesis; (G,H) Metaphase I; (I,J) End of Anaphase II. u: univalent; *: rod bivalent. Scale bars = 5 μm
(K) Quantification of the number of chiasma that can be identified at metaphase I (minimum chiasma number, MCN) in both *asy4* mutants as well as in a series of mutants and multi-mutants. Numbers give the average MCN per cell. The detailed data set can be found in SupData_4.

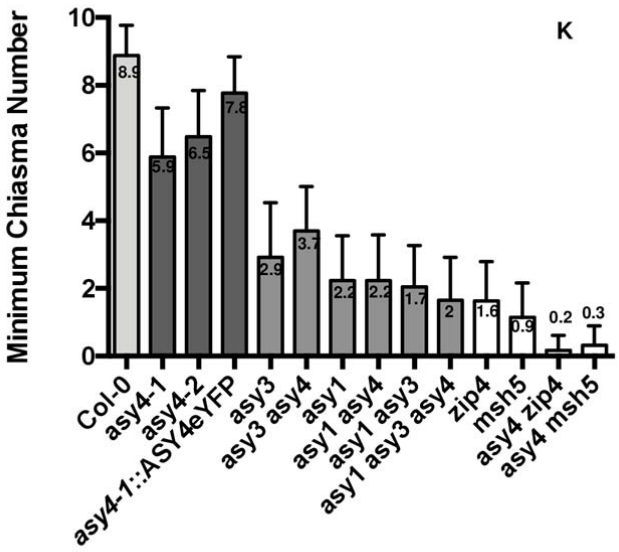

chiasma on a single chromosome arm pair whereas ring bivalents reflect the occurrence of at least one chiasma per chromosome arm. This estimation provides a minimum chiasma number (MCN, as defined in (Jahns et al., 2014)), because multiple chiasmata on a single bivalent arm cannot generally be discriminated from single chiasma. In both *asy4* mutants MCN is significantly decreased in comparison to wild type, with the *asy4-1* allele being the most affected, showing an average of 5.9 ± 1.5 MCN/cell (in wild type the mean number of MCN per cell is 8.9 ± 0.89, t test $P<0.0001$) (Figure 2 and SupData_4). In consequence, all subsequent analyses were conducted with *asy4-1*.

This phenotype of a decrease in chiasma formation associated with abnormal synapsis has previously been described for mutants defective in axis formation typified by *asy1* and *asy3* (Armstrong et al., 2002; Ferdous et al., 2012). We therefore analysed the epistatic relationships between these various mutations. This revealed that, in terms of chiasma level, the *asy1* mutation is epistatic to *asy3* and *asy4*, with *asy1 asy3* and *asy1 asy4* double mutant combinations showing only 2 MCN/cell (Figure 2, and SupData_4). When analysing the double mutant *asy3 asy4* however, we found that the average number of chiasmata per cell is intermediate between *asy3* and *asy4* (4.1±1.3 MCN/cell) and significantly different from each single mutant (one-way ANOVA, $P<0.0005$).

asy4 mutants are defective in meiotic recombination

In order to understand the origin of the reduced chiasma formation observed in *asy4*, we investigated meiotic recombination in further detail. First, we immunolocalised DMC1, a meiosis-specific recombinase, that forms foci at recombination sites. In wild type, DMC1 foci appear at late leptotene/early zygotene reaching an average of 240 foci per nucleus (Chelysheva et al., 2007). In *asy4-1*, we counted an average of 222 ± 107 (n=15) foci per cell suggesting that early recombination events are not affected in *asy4* (SupData_5). We then immunolocalised the ZMM proteins MSH5, the MutS homolog, that is involved in the stabilization of progenitor double-Holliday Junctions and HEI10 which has been shown to mark a subset of recombination intermediates that are channelled into the ZMM pathway (Snowden et al., 2004; Higgins et al., 2008; Chelysheva et al., 2012). MSH5 foci were detected in both wild type and *asy4-1 at* late leptotene/early zygotene (Figure 3, A-B). No significant difference in the number of foci was observed (wild type = 110.9 ± 38.61, n=15; *asy4-1* = 121.1 ± 29.55, n=15; Mann-Whitney U test, P = 0.3835). This implies that recombination in *asy4-1* progresses beyond DMC1 catalysed strand-invasion. HEI10 is loaded early during prophase I on a large number of recombination sites, forming foci of different sizes on chromosomes. As meiosis progresses, HEI10 foci become brighter and associated with the central element of the SC (ZYP1) (Figure 3C). During pachytene a limited number of these foci remain at sites that correspond to class I COs where they co-localise with MLH1 until the end of prophase (not shown). In *asy4-1,* the HEI10 dynamics was similar as in wild type, with mixed sized foci co-localising with

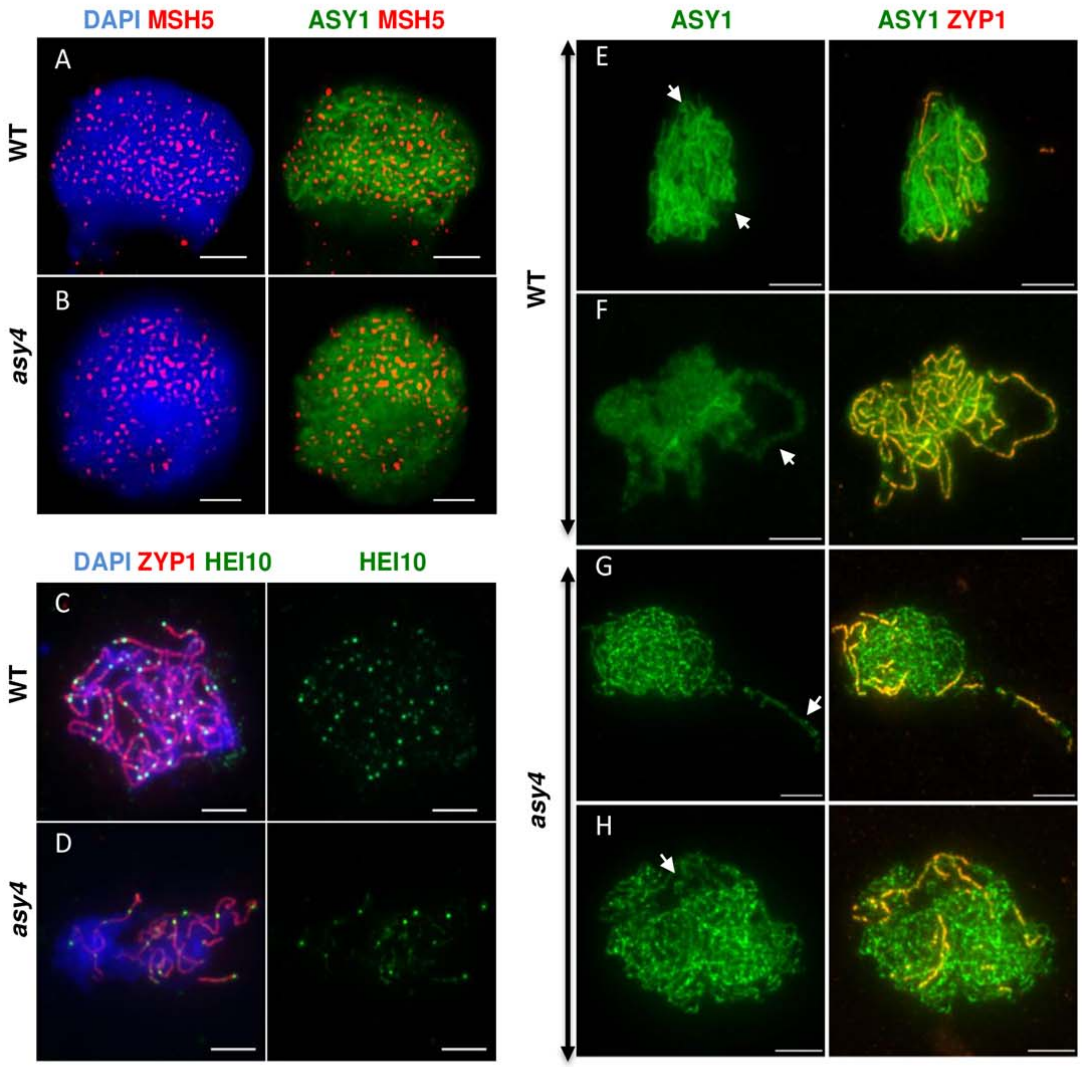

Figure 3: *asy4* mutant is defective in recombination, axis biogenesis and synapsis.
A-B: Dual ASY1 and MSH5 immuno-detection. ASY1(green), MSH5 (red), DAPI (blue). Images are a single frame from mid Z-stack. Scale bars = 2 μm
C-D: Dual ZYP1 and HEI10 immuno-detection together with DAPI (Blue) on male meiocytes at comparable stage. Scale bars = 2 μm
E-H: Dual ASY1 (green) and ZYP1 immuno-detection (red).
Arrows indicate synapsed regions where ASY1 is depleted in wild type but not in *asy4-1*. Scale bars = 2 μm

212 ZYP1 while synapsis progresses (Figure 3D). However, ZYP1 staining was very
213 limited, never progressing to full synapsis, confirming the chromosome synapsis

defects detected after DAPI staining of the chromosomes (Figure 2). In consequence, the pachytene-like HEI10 foci observed on the partially synapsed nuclei were strongly decreased in comparison to wild type (Figure 3D).

We then analysed the level of recombination in four genetic intervals located on chromosome 5 using the Fluorescent Tagged Lines (FTL) tool developed by Copenhaver et al. (Berchowitz et Copenhaver, 2008). For most intervals (3 out of 4) recombination rates decrease significantly but moderately in *asy4*, reaching on average 75% of the wild-type level of recombination (Table 1). This effect is comparable to the decrease in chiasma number observed in *asy4* (Figure 2). However, the I5b interval, which is distally located on chromosome 5, appears differentially affected since meiotic recombination increases slightly but significantly in *asy4* (from 16 to 20 cM) (Table 1). In conclusion, *asy4* mutation provokes a decrease in meiotic recombination, but this effect appears to vary according to the chromosomal intervals considered.

In *A. thaliana,* most COs (85%) exhibit interference. From the FTL data, we estimated the level of interference between COs in each interval by calculating the ratio between the observed number of double COs to the expected number of double COs under the hypothesis of no interference (NPD ratio as defined by (Snow, 1979)). We observed that in most intervals considered, in *asy4* as in wild type, the NPDr is smaller than 1, revealing the presence of interference between adjacent COs. Then the interference between COs occurring in adjacent intervals (I5a/I5b or I5c/I5d) was estimated by calculating the interference ratio (IR) as defined by Malkova et al. (Malkova et al., 2004). The IR compares the genetic length of one interval with and without the presence of a simultaneous event in the neighbouring interval. When the occurrence of a CO in one interval reduces the probability of a CO occurring in the adjacent interval, the IR is less than 1, indicating CO interference. When COs in the two adjacent intervals are independent of each other, the IR is 1, and if the presence of one CO in an interval increases the probability of an additional CO in the adjacent interval, the IR is greater than 1, indicating negative interference. IRs revealed the presence of interference between COs in wild type (for both pairs of intervals) and for *asy4* for the I5c/I5d pair of intervals (Table 1). However, for the I5a/I5b pair of

intervals, the IR in *asy4* is above 1, suggesting that in that chromosomal region adjacent COs occur more frequently than in wild type.

In wild-type *Arabidopsis*, the majority of COs (85%–90%) depend on the ZMM proteins (MSH4, MSH5, MER3, ZIP4, SHOC1/ ZIP2, HEI10, and PTD) as well as on MLH1 and MLH3 (Mercier et al., 2015). We analysed chiasma frequencies in *asy4 zip4* and *asy4 msh5* double mutants (Figure 2). In both cases, the level of bivalent formation was dramatically reduced by more than 95%, showing that almost all the COs in *asy4* are ZMM-dependent. We then estimated the average number of these class I COs in *asy4* mutant by immuno-labelling chromosomes with antibodies directed against MLH1, a marker of class I COs (Figure 4). We found that *asy4-1* shows a limited but significant decrease in MLH1 foci from 11 ± 1.5 (mean ± SD; n=60) in wild type to 8.6 ± 2.2 (n=147) in *asy4-1* (t-test, $P<0.05$), confirming the above genetic results that *asy4* mutation decreases CO formation. We then analysed the distribution of these foci within bivalents. We kept in our analysis all pairs of chromosome arms where at least one MLH1 foci can be observed at diakinesis. In wild-type meiocytes the mean number of MLH1 foci per chromosome arm is 1.4 ± 0.52 (n=180) (range 1-3) whereas in *asy4-1* it increased highly significantly ($P<0.0001$, t test) to a mean of 1.8 ± 0.85 (n=134), with a much greater range of values than in wild type (1- 6 compared to 1-3 in wild-type). These cytological data are in agreement with the FTL analyses and show that *asy4* mutation perturbs meiotic recombination quantitatively (by decreasing it) and qualitatively (by altering CO location).

asy4 mutation is associated with axis defects

We investigated the behaviour of several components of the meiotic chromosome axis (ASY1, ASY3, REC8 and SCC3) in the *asy4* mutant in comparison to wild type (Figure 3, Figure 5, and SupData_6). ASY1, ASY3, REC8 and SCC3 are detected during meiotic prophase I and exhibit different dynamics as meiosis progresses (Armstrong et al., 2002; Cai et al., 2003; Chelysheva et al., 2005; Ferdous et al., 2012). At leptotene, all these proteins brightly decorate meiotic chromosomes, revealing the typical thread-like chromosomal axis. As synapsis proceeds and the central element connects the axial elements of the homologous chromosomes, ASY1

Figure 4

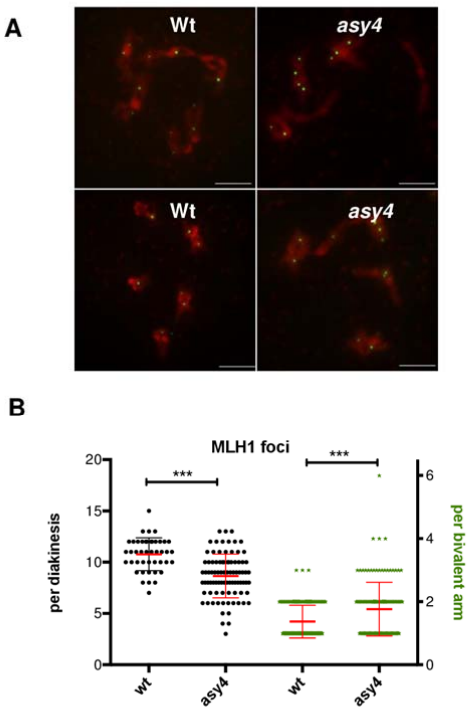

Figure 4 : MLH1 detection and quantification.
(A) MLH1 was immunolocalised (green) on diakinesis chromosomes from wild-type (wt) or *asy4-1* (*asy4*) mutant. Chromosomes were stained by DAPI (red). Scale bars = 5 μm
(B) Average number of MLH1 foci per cell (black) or per bivalent arm (green).

281 is depleted from the axis and consequently the ASY1 signal appears faint and fuzzy
282 (Figure 3 arrows, SupData_6). ASY3, REC8 and SCC3 also mark the chromosome
283 axes, but contrary to ASY1, they are not removed during synapsis (Figure 5 and
284 SupData_6). In the case of the cohesins REC8 and SCC3, no obvious modification in
285 their pattern could be detected (Figure 5 and SupData_6). The two axis-associated

proteins ASY1 and ASY3 are loaded onto the chromosome axis and chromosome threads typical of leptotene stages can be seen. However, ASY1 and ASY3 signals adopt an abnormally patchy and lumpy aspect (Figure 3 and Figure 5), suggesting that in *asy4*, the meiotic chromosome axis is aberrantly structured. In addition, we observed no displacement of ASY1 from the synapsed chromosome axes (Figure 3),

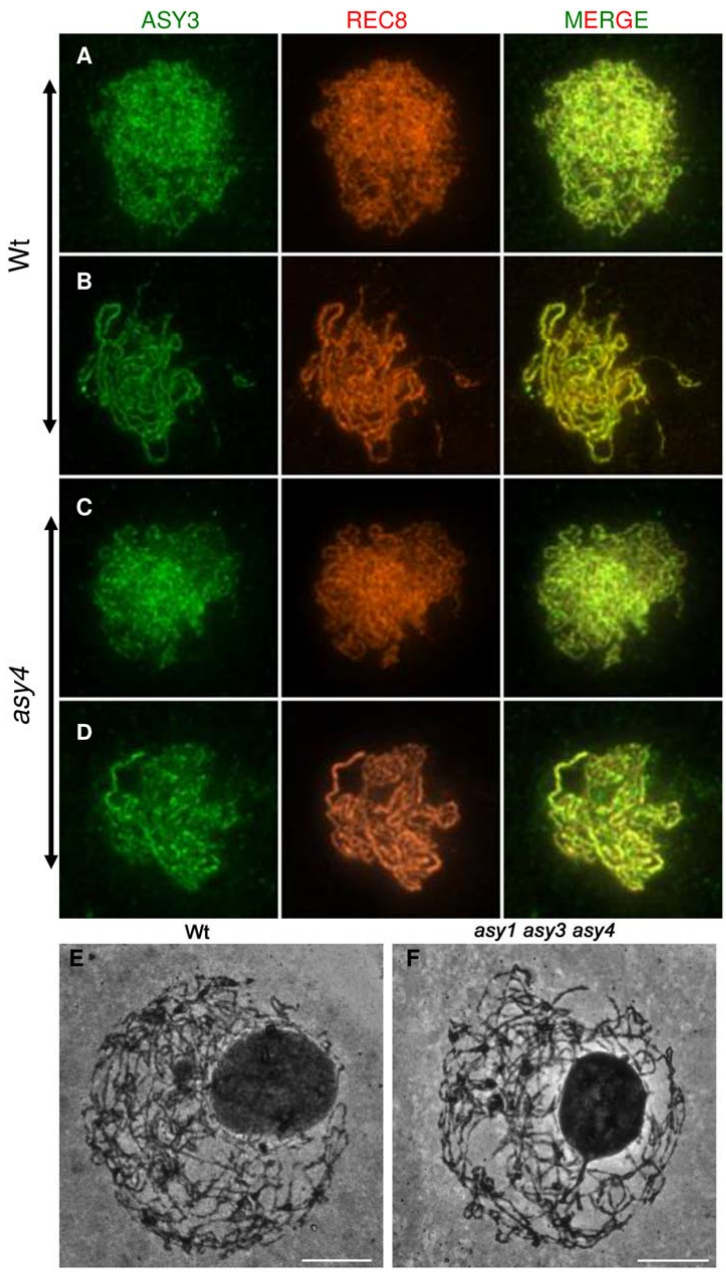

Figure 5 : Chromosome axis investigation
(A-D) Dual ASY3 (green) and REC8 (orange) immunolocalisation on wild-type (A,B) or *asy4-1* mutant (*asy4*) (C,D) male meiocytes. (E,F) Silver staining of wild-type (wt) and triple *asy1asy3asy4* mutant male meiocytes. Scale bars = 2 µm

revealing abnormal axis dynamics. We investigated the chromosome axis further by silver-staining of chromosome spreads and wild-field microscopy observation as described in (Armstrong and Jones, 2001). This chromatin staining permits the detection of the meiotic chromosome axis from leptotene to the end of meiosis. In the *asy4* mutant but also in *asy3 asy4* and *asy1 asy3 asy4,* no modification of the silver-

stained axis could be detected (Figure 5), suggesting that even if axis composition and/or dynamics is affected in *asy4*, at this level of resolution the overall structure of the axis appears physically intact.

ASY4 is an axial-associated protein

To examine the cellular localisation of ASY4 we used fluorescent protein tagging. An ASY4-eYFP construct was produced and introduced into homozygous *asy4-1* plants, the most severely affected mutant background. Seed counts were performed on siliques from T2 generation plants (SupData_7). Fertility levels across the transformant lines were wide ranging, from those comparable to *asy4-1,* to a line that was not significantly different to wild-type (line 165.15, subsequently referred to as *asy4-1*::ASY4eYFP; SupData_7). Analysis of DAPI-stained chromosome spreads of *asy4-1*::ASY4eYFP male meiocytes from T3 plants at metaphase I revealed a chiasma frequency of 7.7 ± 1.1 (n=75). This was significantly higher than *asy4.1* (5.9 ± 1.43 (n= 64); Mann-Whitney U test, $p<0.01$). However, it was slightly lower than wild-type (8.6 ± 0.83 (n=28); (Mann-Whitney U test, $p<0.01$)) (Figure 2, SupData_7). In addition, occasional seed gaps in its siliques were apparent, suggesting that fertility was not completely restored (SupData_7).

Examination of the anthers from *asy4-1*::ASY4eYFP using epi-fluorescence microscopy confirmed expression of the tagged gene within male meiocytes (SupData_7). Localization of ASY4eYFP was then investigated in prophase I chromosome spread preparations by direct fluorescence combined with immuno-staining of the chromosome axis protein, ASY1 and the SC protein, ZYP1. This revealed that ASY4 localises as a linear, axis-associated signal at leptotene where it follows the localisation pattern of ASY1 with alternating regions of high and low intensity (Figure 6). However, in contrast to ASY1 which becomes depleted from the axes as zygotene progresses, it persists on synapsed regions of the chromosomes (Figure 6). In this respect, its behaviour is similar to that of ASY3, REC8 and SCC3.

Considering the similarity between the ASY3 and ASY4 protein sequences, the axial association of these two proteins ((Ferdous et al., 2012) and this study), and the perturbed ASY1 and ASY3 signals observed in *asy4*, we investigated whether these

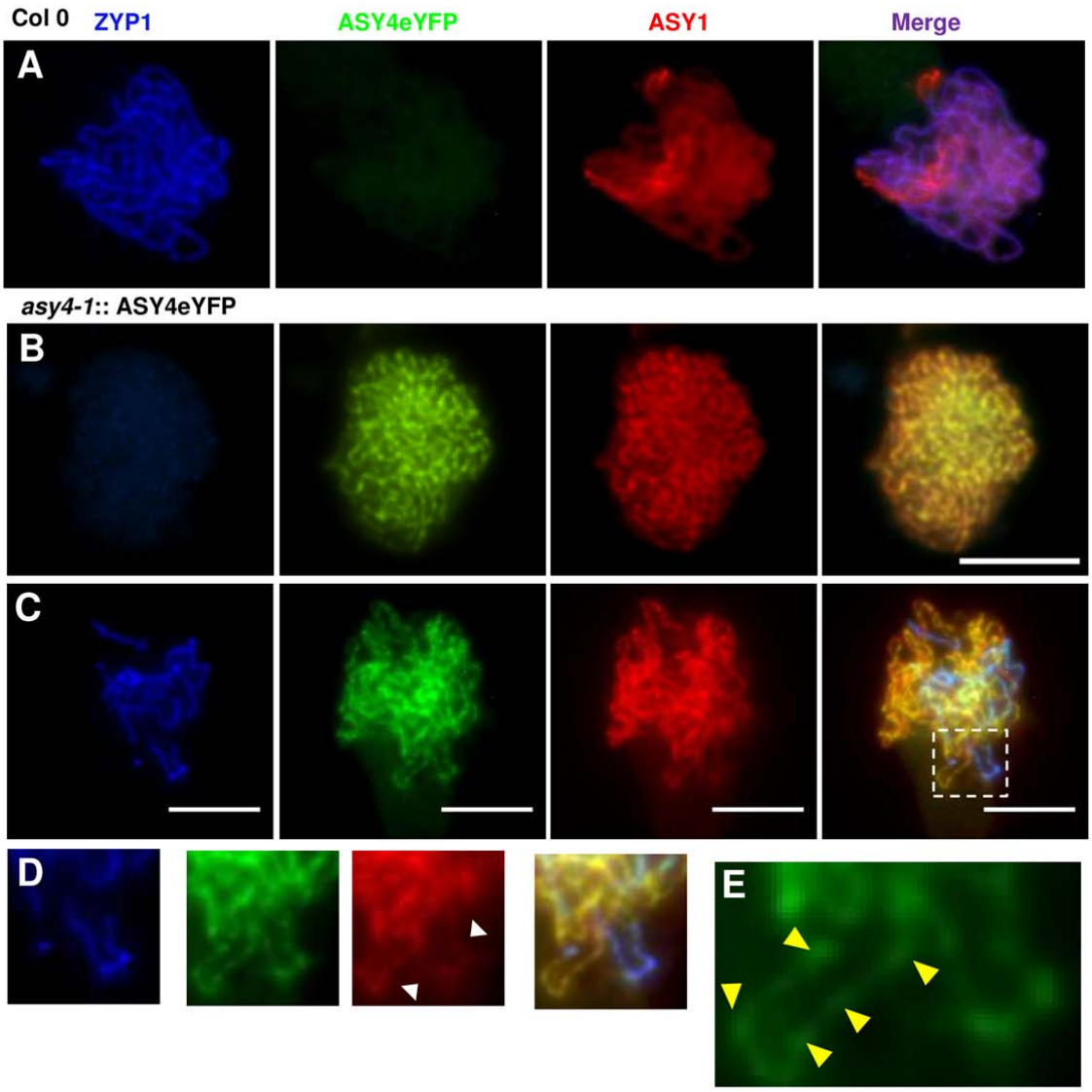

Figure 6: Localization of ASY4eYFP in prophase I chromosome spreads of *asy4-1*::ASY4eYFP. (A) Wild-type (Col 0) zygotene showing absence of eYFP fluorescence. (B) *asy4*-1::ASY4eYFP leptotene and (C) *asy4*-1::ASY4eYFP zygotene . (D) Detail shows the ASY4eYFP fluorescence present on the axis in regions of intense ASY1 staining (unsynapsed) and ZYP1 staining (synapsed). Note reduction in intensity of ASY1 signal in synapsed regions (white arrows). (E) ASY4eYFP fluorescence is not uniform and alternates between regions of high (arrowed) and low intensity. ZYP1 (blue), and ASY1 (red) immunostaining with ASY4-eYFP fluorescence (green). Scale bars = 5µm

proteins physically interact. Interaction between ASY1 and ASY3 has already been demonstrated for *Brassica oleracea* and *Arabidopsis* proteins either *in planta* by co-immunoprecipitation of ASY3 from anthers by antibodies directed against ASY1 or in yeast two hybrid (Y2H) experiments using the *A. thaliana* proteins (Ferdous et al.,

Figure 7

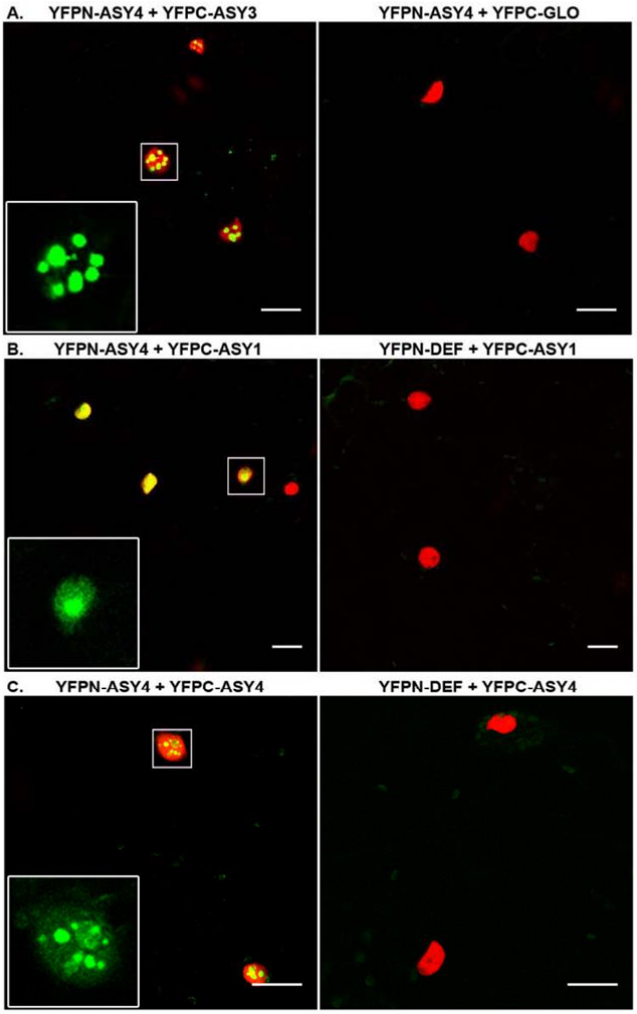

Figure 7: Split-YFP assays in *N. benthamiana* epidermal cells.
N. benthamiana epidermal cells were co-infiltrated with *Agrobacterium* cultures expressing two complementary YFP fusions (N or C-terminal truncations, YFPN or YFPC). Nuclei are identified thanks to a constitutively-expressed fluorescent nuclear protein (H2B-CFP, here shown in red). Interaction between the two tested proteins revealed a YFP signal (green). For each interaction tested, a negative control corresponding to the co-infiltration of one of the fusion protein of interest with the complementary YFP moiety fused with an unrelated protein (*Anthirrinum majus* MADS box transcription factors DEFICIENS -DEF- or GLOBOSA –GLO-). The complete set of split-YFP data can be found in SupData_8. Scale bars = 25 µm

2012). Here, we used bimolecular fluorescence complementation assays in leaf epidermal cells of *Nicotiana benthamiana* plants (BiFC) (Hu et al., 2002). Fusion proteins with complementary YFP truncations (YFP^N + YFP^C) were co-infiltrated in *N. benthamiana* leaves expressing a CFP nuclear marker. As shown in Figure 7 and

SupData_8, this assay revealed interactions among the three ASY proteins and also self-interaction of these three proteins. The YFP signal recovered in these experiments using ASY3 or ASY4 fusion proteins revealed non-uniform nucleus-targeted signals, suggesting that these proteins when overexpressed in plant cells form nuclear aggregates. Y2H experiments confirmed ASY3/ASY4 interactions as well as ASY3/ASY3 and ASY4/ASY4 self-interactions (SupData_9).

345

Discussion

Identification of a new component of the meiotic chromosome axis

We identified the ASY4 protein that shows sequence similarity with the ASY3 C-terminal region and that is closely related with two of the known plant axial components, ASY1/PAIR2 and ASY3/PAIR3/DSY2. The three proteins interact together and ASY4 is required for normal loading and/or stabilisation of ASY1 and ASY3 onto chromosomes. We also found that an ASY4-eYFP fusion protein is axis-associated, leading us to conclude that ASY4 is a new component of the meiotic chromosome axis.

The link between ASY3 and ASY4 can be viewed as a parallel with those existing between the mammalian SYCP2/SCP2 and SYCP3/SCP3: ASY3 and SYCP2/SCP2 are large proteins that show limited sequence similarities with the small coiled-coil proteins ASY4 and SYCP3/SCP3 respectively (as an example SCP3 shows 19% aa identity and 47% aa similarity with the last 163 aa of SCP2); ASY3 and ASY4 interact together (this study) as well as the mammalian SYCP3 and SYCP2 (Yang et al., 2006); all these proteins are axial associated proteins (Offenberg et al., 1998; Schalk et al., 1998; Yang et al., 2006; Ferdous et al., 2012) (this study). In addition, limited sequence similarities can be detected between ASY3/SYCP2 and the *S. cerevisiae* Red1 axial component (Offenberg et al., 1998; Ferdous et al., 2012). The close interconnection between these proteins and the HORMA domain-containing proteins ASY1 in plants (this study and (Wang et al., 2011; Ferdous et al., 2012; Lee et al., 2015)) and HormaD1 and D2 in mammals (Wojtasz et al., 2009) suggests that all together they form a protein complex crucial for the biogenesis of the meiotic chromosome axis scaffold. Taken together these data suggest that ASY3/ASY4 are the functional homologues of the mammalian SYCP2/SYCP3. It is interesting to note that these proteins of the AE as well as those that form the CE of the SC are very poorly conserved at the sequence level but all show the same structure and assembly characteristics (Fraune et al., 2016). This limited sequence conservation among SC proteins from different species is probably due to rapid sequence divergence as has been observed for plant and mammalian SC proteins (Ferdous et al., 2012; Fraune et al., 2016).

ASY4 is required for normal meiotic recombination

According to chiasma and MLH1 counting and to genetic measurement of recombination using FTL lines, CO formation is reduced by a factor of 1.5 in *asy4* mutants. This was correlated with a clear decrease in HEI10 and MLH1 foci at late prophase I and diakinesis, showing that ASY4 is required for normal recombination. It should be noted that the CO decrease observed in *asy4* is lower than the one associated with disruption of either of the two ASY4 partners, ASY1 and ASY3. In terms of chiasma level, the *asy1* mutation is the most affected and is epistatic to *asy3* and *asy4*. This suggests that among the three axis components ASY1, ASY3 and ASY4, the HORMA-domain containing protein ASY1 is a key player, while ASY3 and ASY4 could be seen as accessory proteins. Nevertheless, we cannot exclude the possibility that the partially penetrant phenotype of *asy4* is due to leaky mutations since we could detect the transcription of the 5' end of the gene in both mutants.

Interestingly we observed that the decrease in recombination observed in *asy4* mutants is differentially distributed within the genome since we found that one interval out of four tested (I5b) revealed an increase in CO level (from 16 to 20 cM). This could be related to the distal location of this interval on chromosome 5 and to the observation that the vast majority of chiasma are terminally-located in *asy3* and *asy1* mutants (Ross et al., 1997; Ferdous et al., 2012). Two other findings of our study confirm that CO location is modified in *asy4*. First, despite the average decrease in MLH1 foci in *asy4* mutants, we detected an increased number of MLH1 foci per chromosome arm in comparison to wild type, with up to 6 foci in the same arm while we have never observed more than 3 per chromosome arm in wild type. Second, we found an interference ratio greater than 1 for one pair of intervals tested by FTL (I5a/I5b). This latter result involves the I5b terminally located interval on chromosome 5, suggesting that the two phenomena may be connected and that, in *asy4*, COs are not only decreased but also tend to group in the distal parts of the chromosomes. In this regard, it is interesting to note that we reported recently that, in *Arabidopsis* as in most species, synapsis is preferentially initiated from the distal parts of the chromosomes (Hurel et al. Plant J. in press). If this is also the case in *asy4*, the limited number of ZYP1-labelled central elements on which recombination events appear to be restricted (according to HEI10 labelling, Figure 3) are expected to be predominantly distally located. This could explain why we observed a bias in location of the COs in *asy4*. Further studies will be required to confirm these observations genome-wide and to understand the mechanisms involved.

According to our study, the decrease in CO formation measured in *asy4* is not correlated with a decrease in the overall number of early initiation events since the number of DMC1 and MSH5 foci was unchanged in *asy4-1* in comparison to wild type. It is interesting to note that the role in recombination of the three ASY proteins can be differentiated: ASY1, like ASY4, is not required for normal DSB formation but, contrary to ASY4, is mandatory for the formation of stable DMC1 nucleofilaments (Sanchez-Moran et al., 2007) while ASY3 is required at the step of DSB formation (Ferdous et al., 2012). Chromosome fragmentation was not detected in *asy4,* showing that the DMC1-labelled recombination events are eventually repaired, either using the sister chromatid or the homologous chromosome as a template. Since the number of MSH5 foci at early/mid prophase I appeared normal in *asy4-1*, it would seem likely that recombination proceeds beyond the initial strand invasion stage. This would imply that CO designation, which occurs in early prophase I (Lambing et al., 2017), is normal in the mutant but that a proportion of the designated intermediates fail to mature into COs, consistent with the observed reduction in MLH1 and HEI10 foci. The defect in SC polymerization observed in *asy4* may result in CO designated recombination intermediates that lie within regions of the homologs that remain aysynaptic failing to form COs. Establishing the exact relationship between the loss of ASY4 and the defect in SC formation will be the target of future investigation.

Materials and Methods

Plant material and growth conditions

asy4-1 (SK22114, CS1006148) was available in the public databases and was provided by the NASC (http://arabidopsis.info/) (Scholl et al., 2000). *asy4-2* (line 65433) was identified through a PCR-based screen of the Koncz's collection (Ríos et al., 2002). Other mutant alleles used in this study are *asy1* (SALK_046272, N546272), *asy3* (SALK_143676, N643676), *dmc1* (SAIL_170_F08, N871769), *mer3* (SALK_091560, N591560), *mlh1* (SK25975, N1008089), *msh5* (SALK_026553, N526553), *rad51* (GABI_134A01) and *zip4* (SALK_068052, N568052). Genotyping conditions and primer sequences are given in SupData_10 and SupData_11).

Arabidopsis thaliana and *Nicotiana benthamiana* plants were grown in the greenhouse (photoperiod 16 h/day and 8 h/night; temperature 20°C day and night; humidity 70%; photoperiod 13 h/day and 11 h/night; temperature 25°C day and 17°C night, respectively).

Clone construction

ASY4 cDNA was amplified on flower bud cDNA (Col-0) after two rounds of nested PCR (PCRI: AtASY4RTF and AtASY4RTR, PCRII: AtASY4attB1and AtASY4attB2, SupData_10) and cloned into pDONR207 (Invitrogen) following the manufacturer's instructions. The generated entry vector was sequenced and used to transfer ASY4 cDNA into the yeast two hybrid expression vectors pDEST-GADT7 and pDEST-GBKT7 (Rossignol et al., 2007). To generate the C-terminus Split-YFP clones (Azimzadeh et al., 2008), a version of the cDNA without a STOP codon was amplified beforehand using primers AtASY4attB1 and AtASY4-attB2wostop (SupData_10). Similar approaches were undertaken for ASY1 and ASY3 cDNAs except that using primers AtASY1-attB1, AtASY3-attB1, AtASY3-attB2, AtASY3-attB2wostop, and AtASY1-attB2 (SupData_10).

Yeast two hybrid

Yeast two hybrid assays were carried out using the GAL4-based system (Clontech). SV40 Antigen T (AgT) and p53 protein were used as positive controls. Yeast

plasmids were introduced in AH109 or Y187 strains by lithium acetate transformation following the protocol in the MATCHMAKER GAL4 Two hybrid System 3 manual (Clontech). After mating in appropriate pairwise combinations, the resulting diploids cells were selected on SD medium lacking a combination of amino acids, driven by the auxotrophy genes carried by the cloning vectors. Protein interactions were assayed by growing diploid cells on SD-LWH, and SD-LWHA.

Bimolecular fluorescence complementation

Protein interactions were tested *in planta* using bimolecular fluorescence complementation (BiFC) assays (Hu et al., 2002) in leaf epidermal cells of *N. benthamiana* plants expressing a nuclear cyan fluorescent protein (CFP fused to histone 2B) (Martin et al., 2009). For each protein, four expression vectors were produced, generating inactive N- or C-termini of the YFP (YFP^N, YFP^C) fused with the target sequence in N- or C-termini. Combinations bringing together the two YFP complementary regions (YFP^N + YFP^C) were co-infiltrated in *N. benthamiana* leaves as described in (Azimzadeh et al., 2008; Vrielynck et al., 2016).

Bioinformatics

PSI BLAST on nr database using ASY3 as a query picked up at the first round of iteration At2g33793 with its C terminal region (aa 636-777, where coiled coils lie (aa 625-785, according to (Ferdous et al., 2012)). BLASTP and TBLASTN on plant sequenced genomes present in phytozome 12 database (Blosum45) were done to identify for homologues.

Recombination measurement

We used the fluorescent-tagged lines (FTLs) described in (Berchowitz and Copenhaver, 2008) to estimate recombination rates in four different genomic intervals (I5a, I5b, I5c and I5d). We generated plants that were homozygous for the *qrt* mutation, heterozygous for pairs of linked fluorescent markers RY/++ (I5a and i5d) or YC/++ (I5b and I5c) (R red, Y yellow, C Cyan) and either wild type or homozygous for the *asy4-1* mutation. Tetrad analyses were carried out as described in (Berchowitz and Copenhaver, 2008) on tetrads where each fluorescent marker segregated correctly.

Fluorescent protein tagging

The ASY4 genomic locus, comprising 1835 base pairs upstream of the start codon to 502 base pairs downstream of the stop codon and including all introns and UTRs, was amplified with the primers At2g33793-P9 and At2g33793-P10 (SupData_10). The eYFP sequence was inserted in frame at amino-acid position 202, downstream of the predicted coiled-coil region and close to the C-terminus. The construct was inserted into p35-Nos-BM cloning vector using *Sfi* I sites incorporated into the primers. The resulting expression cassette was subcloned via *Sfi* I into pLH9000 binary vector and used for Agrobacterium-mediated transformation of plants using floral dip. Transformants were selected on kanamycin (50 µg/ml) Murashige and Skoog media (Murashige and Skoog, 1962).

Cytological procedures

Meiotic chromosome spreads were DAPI stained as described previously in (Ross et al., 1996) or silver nitrate stained as described in (Armstrong et al., 2001). Immunostaining of male meiotic spreads was carried out as in (Armstrong and Osman, 2013; Chelysheva et al., 2013). Antibodies used for immunolocalisation were anti-ASY1 (rat, 1 in 1000 dilution) (Armstrong et al, 2002), anti-AtZYP1 (rabbit, N-terminus Ab aa residues 1-415, 1 in 500 dilution) (Higgins et al., 2005), anti-ASY3 (rabbit, 1 in 250 dilution) (Ferdous et al., 2012), anti-REC8 (rat, 1 in 250 dilution) (Cromer et al., 2013), anti-DMC1 (rat, 1 in 20 dilution) (Vignard et al., 2007), anti-MSH5 (rabbit, 1 in 200 dilution) (Higgins et al., 2008), anti-MLH1 (rabbit, 1 in 200 dilution) (Chelysheva et al., 2013) and anti-HEI10 (rabbit, 1 in 250 dilution) (Chelysheva et al., 2012).

Image analysis

asy4-1::ASY4eYFP zygotene male meiocyte nucleus image was captured with Nikon 90i, 100x objective as a Z-stack. The green channel (eYFP) was processed as an average intensity projection using Fiji, due to more rapid bleaching of eYFP relative to the red (Texas red-ASY1) and blue (Alexa350-ZYP1) channels, which were processed as maximum intensity projections. Col-0 was imaged using the same exposure times and processed in the same way. MSH5 foci were scored using Z-stack images and ‘Mexican Hat’ deconvolution as described in (Ferdous et al., 2012).

Ackowledgements:

We wish to thank Christine Mézard for critical reading of the manuscript. The IJPB benefits from the support of the LabEx Saclay Plant Sciences-SPS (ANR-10-LABX-0040-SPS). We also thank Csaba Koncz and Sabine Schäfer for giving access to the MPIPZ T-DNA insertion mutant collection.

One-sentence summary:

A new component of the meiotic chromosome axis is required for normal meiotic recombination and synapsis in *Arabidopsis thaliana*.

Authors' contributions: A.C., A.D., K.O. and A.W. performed most of the experiments; D.V., C.H., L.C., A.R. and S.H. provided technical assistance, A.D.M., F.C.H.F. and M.G. conceived the experiments, F.C.H.F. and M.G. supervised the writing.

Funding information:

F.C.H.F. laboratory: BBSRC grant numbers ERA-Caps-13 BB/M004902/1 and MIBTP GBGB.GAM2526.

Present addresses:

S.H.: Leibniz Institute of Plant Genetics and Crop Plant Research (IPK), Stadt Seeland, Germany.

A.D.M.: Institut Curie, PSL Research University, CNRS, UMR3664, F-75005, Paris, France.

A.W.: Central European Institute of Technology, Masaryk University, Kamenice, 753/5, 62500, Czech Republic.

A.R.: Instituto de Biotecnologia / UNAM, Av. Universidad #2001, Col. Chamilpa C.P. 62210, Cuernavaca, Morelos, MEXICO.

Corresponding author email: mathilde.grelon@inra.fr

Tables

Table 1:

	interval	Nb of tetrads	d (cM)	d ratio (asy4/wt)	NPD ratio	IR
wt	i5a	10,303	27	-	0.3**	0.4**
	i5b	10,303	16.1	-	0.2**	
	i5c	14,590	7.7	-	0.3**	0.3**
	i5d	14,590	7.4	-	0.3**	
asy4-1	i5a	7,462	15.5	0.6	0.9	1.2**
	i5b	7,462	20	1.2	0.6**	
	i5c	13,753	6.8	0.9	0.4**	0.7**
	i5d	13,753	5.6	0.8	0.5*	

Figure Legends:

Figure 1: Schematic representation of ASY4 protein and gene.

A. The ASY4 protein shows similarities with ASY3 C-terminal region (dashed lines). Predicted coiled-coils of both proteins are indicated by grey boxes.

B. *ASY4* open reading frame and position of the T-DNA insertion in *asy4-1* and *asy4-2* mutants. Exons are shown as grey boxes.

Figure 2: ASY4 is required for normal meiosis.

(A-J) DAPI staining of meiotic chromosomes in wild type (A,C,E,G,I) and *asy4-1* (B,D,F,H,J). (A,B) Leptotene; (C) Pachytene; (D) Partial synapsis typical of the defects of synapsis observed in *asy4* mutants; (E,F) Diakinesis; (G,H) Metaphase I; (I,J) End of Anaphase II. u: univalent; *rod bivalent. Scale bars = 5 μm

(K) Quantification of the number of chiasma that can be identified at metaphase I (minimum chiasma number, MCN) in both *asy4* mutants as well as in a series of mutants and multi-mutants. Numbers give the average MCN per cell. The detailed data set can be found in SupData_4.

Figure 3: asy4 mutant is defective in recombination, axis biogenesis and synapsis.

A-B: Dual ASY1 and MSH5 immuno-detection. ASY1(green), MSH5 (red), DAPI (blue). Images are a single frame from mid Z-stack. Scale bars = 2 μm

C-D: Dual ZYP1 and HEI10 immuno-detection together with DAPI (Blue) on male meiocytes at comparable stage. Scale bars = 2 μm

E-H: Dual ASY1 (green) and ZYP1 immuno-detection (red). Arrows indicate synapsed regions where ASY1 is depleted in wild type but not in asy4-1. Scale bars = 2 μm

Figure 4: MLH1 detection and quantification.

(A) MLH1 was immunolocalised (green) on diakinesis chromosomes from wild-type (wt) or *asy4-1* (*asy4*) mutant. Chromosomes were stained by DAPI (red). Scale bars = 5 μm

(B) Average number of MLH1 foci per cell (black) or per bivalent arm (green).

Figure 5: Chromosome axis investigation

(A-D) Dual ASY3 (green) and REC8 (orange) immunolocalisation on wild-type (A,B) or *asy4-1* mutant (*asy4*) (C,D) male meiocytes. (E,F) Silver staining of wild-type (wt) and triple *asy1asy3asy4* mutant male meiocytes. Scale bars = 2 μm

Figure 6: Localization of ASY4eYFP in prophase I chromosome spreads of *asy4-1*::ASY4eYFP. (A) Wild-type (Col 0) zygotene showing absence of eYFP fluorescence. (B) *asy4*-1::ASY4eYFP leptotene and (C) *asy4*-1::ASY4eYFP zygotene. (D) Detail shows the ASY4eYFP fluorescence present on the axis in regions of intense ASY1 staining (unsynapsed) and ZYP1 staining (synapsed). Note reduction in intensity of ASY1 signal in synapsed regions (white arrows). (E) ASY4eYFP fluorescence is not uniform and alternates between regions of high (arrowed) and low intensity. ZYP1 (blue), and ASY1 (red) immunostaining with ASY4-eYFP fluorescence (green). Scale bars = 5μm

Figure 7: Split-YFP assays in *N. benthamiana* epidermal cells.

N. benthamiana epidermal cells were co-infiltrated with *Agrobacterium* cultures expressing two complementary YFP fusions (N or C-terminal truncations, YFPN or YFPC). Nuclei are identified thanks to a constitutively-expressed fluorescent nuclear protein (H2B-CFP, here shown in red). Interaction between the two tested proteins revealed a YFP signal (green). For each interaction tested, a negative control corresponding to the co-infiltration of one of the fusion protein of interest with the complementary YFP moiety fused with an unrelated protein (*Anthirrinum majus* MADS box transcription factors DEFICIENS -DEF- or GLOBOSA –GLO-). The complete set of split-YFP data can be found in SupData_8. Scale bars = 25 μm

642

Parsed Citations

Armstrong SJ, Caryl AP, Jones GH, Franklin FCH (2002) Asy1, a protein required for meiotic chromosome synapsis, localizes to axis-associated chromatin in Arabidopsis and Brassica. J Cell Sci 115: 3645-55

Pubmed: Author and Title
CrossRef: Author and Title
Google Scholar: Author Only Title Only Author and Title

Armstrong SJ, Franklin FCH, Jones GH (2001) Nucleolus-associated telomere clustering and pairing precede meiotic chromosome synapsis in Arabidopsis thaliana. J Cell Sci 114: 4207-17

Pubmed: Author and Title
CrossRef: Author and Title
Google Scholar: Author Only Title Only Author and Title

Armstrong SJ, Jones GH (2001) Female meiosis in wild-type Arabidopsis thaliana and in two meiotic mutants. Sex Plant Reprod 13: 177-183

Pubmed: Author and Title
CrossRef: Author and Title
Google Scholar: Author Only Title Only Author and Title

Armstrong SJ, Osman K (2013) Immunolocalization of meiotic proteins in Arabidopsis thaliana: method 2. Methods Mol Biol 990: 103-7

Pubmed: Author and Title
CrossRef: Author and Title
Google Scholar: Author Only Title Only Author and Title

Azimzadeh J, Nacry P, Christodoulidou A, Drevensek S, Camilleri C, Amiour N, Parcy F, Pastuglia M, Bouchez D (2008) Arabidopsis TONNEAU1 proteins are essential for preprophase band formation and interact with centrin. Plant Cell 20: 2146-59

Pubmed: Author and Title
CrossRef: Author and Title
Google Scholar: Author Only Title Only Author and Title

Berchowitz LE, Copenhaver GP (2008) Fluorescent Arabidopsis tetrads: a visual assay for quickly developing large crossover and crossover interference data sets. Nat Protoc 3: 41-50

Pubmed: Author and Title
CrossRef: Author and Title
Google Scholar: Author Only Title Only Author and Title

Blat Y, Protacio RU, Hunter N, Kleckner N (2002) Physical and functional interactions among basic chromosome organizational features govern early steps of meiotic chiasma formation. Cell 111: 791-802

Pubmed: Author and Title
CrossRef: Author and Title
Google Scholar: Author Only Title Only Author and Title

Börner GV, Barot A, Kleckner N (2008) Yeast Pch2 promotes domainal axis organization, timely recombination progression, and arrest of defective recombinosomes during meiosis. Proc Natl Acad Sci U S A 105: 3327-32

Pubmed: Author and Title
CrossRef: Author and Title
Google Scholar: Author Only Title Only Author and Title

Cai X, Dong F, Edelmann RE, Makaroff CA (2003) The Arabidopsis SYN1 cohesin protein is required for sister chromatid arm cohesion and homologous chromosome pairing. J Cell Sci 116: 2999-3007

Pubmed: Author and Title
CrossRef: Author and Title
Google Scholar: Author Only Title Only Author and Title

Chelysheva LA, Grandont L, Grelon M (2013) Immunolocalization of meiotic proteins in Brassicaceae: method 1. Methods Mol Biol 990: 93-101

Pubmed: Author and Title
CrossRef: Author and Title
Google Scholar: Author Only Title Only Author and Title

Chelysheva L, Diallo S, Vezon D, Gendrot G, Vrielynck N, Belcram K, Rocques N, Márquez-Lema A, Bhatt AM, Horlow C, et al. (2005) AtREC8 and AtSCC3 are essential to the monopolar orientation of the kinetochores during meiosis. J Cell Sci 118: 4621-32

Pubmed: Author and Title
CrossRef: Author and Title
Google Scholar: Author Only Title Only Author and Title

Chelysheva L, Gendrot G, Vezon D, Doutriaux M-P, Mercier R, Grelon M (2007) Zip4/Spo22 is required for class I CO formation but not for synapsis completion in Arabidopsis thaliana. PLoS Genet 3: e83

Pubmed: Author and Title
CrossRef: Author and Title
Google Scholar: Author Only Title Only Author and Title

Chelysheva L, Vezon D, Chambon A, Gendrot G, Pereira L, Lemhemdi A, Vrielynck N, Le Guin S, Novatchkova M, Grelon M (2012) The

Arabidopsis HEI10 is a new ZMM protein related to Zip3. PLoS Genet 8: e1002799
Pubmed: Author and Title
CrossRef: Author and Title
Google Scholar: Author Only Title Only Author and Title

Cromer L, Jolivet S, Horlow C, Chelysheva L, Heyman J, De Jaeger G, Koncz C, De Veylder L, Mercier R (2013) Centromeric cohesion is protected twice at meiosis, by SHUGOSHINs at anaphase I and by PATRONUS at interkinesis. Curr Biol 23: 2090-9
Pubmed: Author and Title
CrossRef: Author and Title
Google Scholar: Author Only Title Only Author and Title

Ferdous M, Higgins JD, Osman K, Lambing C, Roitinger E, Mechtler K, Armstrong SJ, Perry R, Pradillo M, Cuñado N, et al. (2012) Inter-homolog crossing-over and synapsis in Arabidopsis meiosis are dependent on the chromosome axis protein AtASY3. PLoS Genet 8: e1002507
Pubmed: Author and Title
CrossRef: Author and Title
Google Scholar: Author Only Title Only Author and Title

Fraune J, Brochier-Armanet C, Alsheimer M, Volff J-N, Schücker K, Benavente R (2016) Evolutionary history of the mammalian synaptonemal complex. Chromosoma 125: 355-60
Pubmed: Author and Title
CrossRef: Author and Title
Google Scholar: Author Only Title Only Author and Title

Higgins JD, Sanchez-Moran E, Armstrong SJ, Jones GH, Franklin FCH (2005) The Arabidopsis synaptonemal complex protein ZYP1 is required for chromosome synapsis and normal fidelity of crossing over. Genes Dev 19: 2488-500
Pubmed: Author and Title
CrossRef: Author and Title
Google Scholar: Author Only Title Only Author and Title

Higgins JD, Vignard J, Mercier R, Pugh AG, Franklin FCH, Jones GH (2008) AtMSH5 partners AtMSH4 in the class I meiotic crossover pathway in Arabidopsis thaliana, but is not required for synapsis. Plant J 55: 28-39
Pubmed: Author and Title
CrossRef: Author and Title
Google Scholar: Author Only Title Only Author and Title

Hu C-D, Chinenov Y, Kerppola TK (2002) Visualization of interactions among bZIP and Rel family proteins in living cells using bimolecular fluorescence complementation. Mol Cell 9: 789-98
Pubmed: Author and Title
CrossRef: Author and Title
Google Scholar: Author Only Title Only Author and Title

Jahns MT, Vezon D, Chambon A, Pereira L, Falque M, Martin OC, Chelysheva L, Grelon M (2014) Crossover localisation is regulated by the neddylation posttranslational regulatory pathway. PLoS Biol 12: e1001930
Pubmed: Author and Title
CrossRef: Author and Title
Google Scholar: Author Only Title Only Author and Title

Lambing C, Franklin FCH, Wang C-JR (2017) Understanding and Manipulating Meiotic Recombination in Plants. Plant Physiol 173: 1530-1542
Pubmed: Author and Title
CrossRef: Author and Title
Google Scholar: Author Only Title Only Author and Title

Lambing C, Osman K, Nuntasoontorn K, West A, Higgins JD, Copenhaver GP, Yang J, Armstrong SJ, Mechtler K, Roitinger E, et al. (2015) Arabidopsis PCH2 Mediates Meiotic Chromosome Remodeling and Maturation of Crossovers. PLoS Genet 11: e1005372
Pubmed: Author and Title
CrossRef: Author and Title
Google Scholar: Author Only Title Only Author and Title

Lee DH, Kao Y-H, Ku J-C, Lin C-Y, Meeley R, Jan Y-S, Wang C-JR (2015) The Axial Element Protein DESYNAPTIC2 Mediates Meiotic Double-Strand Break Formation and Synaptonemal Complex Assembly in Maize. Plant Cell 27: 2516-29
Pubmed: Author and Title
CrossRef: Author and Title
Google Scholar: Author Only Title Only Author and Title

Malkova A, Swanson J, German M, McCusker JH, Housworth EA, Stahl FW, Haber JE (2004) Gene conversion and crossing over along the 405-kb left arm of Saccharomyces cerevisiae chromosome VII. Genetics 168: 49-63
Pubmed: Author and Title
CrossRef: Author and Title
Google Scholar: Author Only Title Only Author and Title

Martin K, Kopperud K, Chakrabarty R, Banerjee R, Brooks R, Goodin MM (2009) Transient expression in Nicotiana benthamiana fluorescent marker lines provides enhanced definition of protein localization, movement and interactions in planta. Plant J 59: 150-62
Pubmed: Author and Title

CrossRef: Author and Title
Google Scholar: Author Only Title Only Author and Title

Mercier R, Mézard C, Jenczewski E, Macaisne N, Grelon M (2015) The molecular biology of meiosis in plants. Annu Rev Plant Biol 66: 297-327
Pubmed: Author and Title
CrossRef: Author and Title
Google Scholar: Author Only Title Only Author and Title

Murashige T, Skoog F (1962) A Revised Medium for Rapid Growth and Bio Assays with Tobacco Tissue Cultures. Physiol Plant 15: 473-497
Pubmed: Author and Title
CrossRef: Author and Title
Google Scholar: Author Only Title Only Author and Title

Offenberg HH, Schalk JAC, Meuwissen RLJ, van Aalderen M, Kester HA, Dietrich AJJ, Heyting C (1998) SCP2: a major protein component of the axial elements of synaptonemal complexes of the rat. Nucleic Acids Res 26: 2572-9
Pubmed: Author and Title
CrossRef: Author and Title
Google Scholar: Author Only Title Only Author and Title

Panizza S, Mendoza MA, Berlinger M, Huang L, Nicolas A, Shirahige K, Klein F (2011) Spo11-accessory proteins link double-strand break sites to the chromosome axis in early meiotic recombination. Cell 146: 372-83
Pubmed: Author and Title
CrossRef: Author and Title
Google Scholar: Author Only Title Only Author and Title

Pattabiraman D, Roelens B, Woglar A, Villeneuve AM (2017) Meiotic recombination modulates the structure and dynamics of the synaptonemal complex during C. elegans meiosis. PLoS Genet 13: e1006670
Pubmed: Author and Title
CrossRef: Author and Title
Google Scholar: Author Only Title Only Author and Title

Pelttari J, Hoja M, Yuan L, Liu J, Brundell E, Moens P, Santucci-Darmanin S, Jessberger R, Barbero JL, Heyting C, et al. (2001) A Meiotic Chromosomal Core Consisting of Cohesin Complex Proteins Recruits DNA Recombination Proteins and Promotes Synapsis in the Absence of an Axial Element in Mammalian Meiotic Cells. Mol Cell Biol 21: 5667-5677
Pubmed: Author and Title
CrossRef: Author and Title
Google Scholar: Author Only Title Only Author and Title

Ríos G, Lossow A, Hertel B, Breuer F, Schaefer S, Broich M, Kleinow T, Jásik J, Winter J, Ferrando A, et al. (2002) Rapid identification of Arabidopsis insertion mutants by non-radioactive detection of T-DNA tagged genes. Plant J 32: 243-53
Pubmed: Author and Title
CrossRef: Author and Title
Google Scholar: Author Only Title Only Author and Title

Ross KJ, Fransz P, Armstrong SJ, Vizir I, Mulligan B, Franklin FCH, Jones GH (1997) Cytological characterization of four meiotic mutants of Arabidopsis isolated from T-DNA-transformed lines. Chromosome Res 5: 551-9
Pubmed: Author and Title
CrossRef: Author and Title
Google Scholar: Author Only Title Only Author and Title

Ross KJ, Fransz P, Jones GH (1996) A light microscopic atlas of meiosis in Arabidopsis thaliana. Chromosome Res 4: 507-16
Pubmed: Author and Title
CrossRef: Author and Title
Google Scholar: Author Only Title Only Author and Title

Rossignol P, Collier S, Bush M, Shaw P, Doonan JH (2007) Arabidopsis POT1A interacts with TERT-V(I8), an N-terminal splicing variant of telomerase. J Cell Sci 120: 3678-87
Pubmed: Author and Title
CrossRef: Author and Title
Google Scholar: Author Only Title Only Author and Title

Sanchez-Moran E, Santos J-L, Jones GH, Franklin FCH (2007) ASY1 mediates AtDMC1-dependent interhomolog recombination during meiosis in Arabidopsis. Genes Dev 21: 2220-33
Pubmed: Author and Title
CrossRef: Author and Title
Google Scholar: Author Only Title Only Author and Title

Schalk JA, Dietrich AJ, Vink AC, Offenberg HH, van Aalderen M, Heyting C (1998) Localization of SCP2 and SCP3 protein molecules within synaptonemal complexes of the rat. Chromosoma 107: 540-8
Pubmed: Author and Title
CrossRef: Author and Title
Google Scholar: Author Only Title Only Author and Title

Scholl RL, May ST, Ware DH (2000) Seed and molecular resources for Arabidopsis. Plant Physiol 124: 1477-80

Pubmed: Author and Title
CrossRef: Author and Title
Google Scholar: Author Only Title Only Author and Title

Snow R (1979) Maximum Likelihood Estimation Of Linkage And Interference From Tetrad Data. Genetics 92: 231-245
Pubmed: Author and Title
CrossRef: Author and Title
Google Scholar: Author Only Title Only Author and Title

Snowden T, Acharya S, Butz C, Berardini M, Fishel R (2004) hMSH4-hMSH5 recognizes Holliday Junctions and forms a meiosis-specific sliding clamp that embraces homologous chromosomes. Mol Cell 15: 437-51
Pubmed: Author and Title
CrossRef: Author and Title
Google Scholar: Author Only Title Only Author and Title

Sun X, Huang L, Markowitz TE, Blitzblau HG, Chen D, Klein F, Hochwagen A (2015) Transcription dynamically patterns the meiotic chromosome-axis interface. Elife 4: 1-23
Pubmed: Author and Title
CrossRef: Author and Title
Google Scholar: Author Only Title Only Author and Title

Syrjänen JL, Heller I, Candelli A, Davies OR, Peterman EJG, Wuite GJL, Pellegrini L (2017) Single-molecule observation of DNA compaction by meiotic protein SYCP3. Elife 6: 1-14
Pubmed: Author and Title
CrossRef: Author and Title
Google Scholar: Author Only Title Only Author and Title

Syrjänen JL, Pellegrini L, Davies OR (2014) A molecular model for the role of SYCP3 in meiotic chromosome organisation. Elife 3: 1-18
Pubmed: Author and Title
CrossRef: Author and Title
Google Scholar: Author Only Title Only Author and Title

Vignard J, Siwiec T, Chelysheva L, Vrielynck N, Gonord F, Armstrong SJ, Schlögelhofer P, Mercier R (2007) The interplay of RecA-related proteins and the MND1-HOP2 complex during meiosis in Arabidopsis thaliana. PLoS Genet 3: 1894-906
Pubmed: Author and Title
CrossRef: Author and Title
Google Scholar: Author Only Title Only Author and Title

Vrielynck N, Chambon A, Vezon D, Pereira L, Chelysheva L, De Muyt A, Mézard C, Mayer C, Grelon M (2016) A DNA topoisomerase VI-like complex initiates meiotic recombination. Science 351: 939-43
Pubmed: Author and Title
CrossRef: Author and Title
Google Scholar: Author Only Title Only Author and Title

Wang K, Wang M, Tang D, Shen Y, Qin B, Li M, Cheng Z (2011) PAIR3, an axis-associated protein, is essential for the recruitment of recombination elements onto meiotic chromosomes in rice. Mol Biol Cell 22: 12-9
Pubmed: Author and Title
CrossRef: Author and Title
Google Scholar: Author Only Title Only Author and Title

Wojtasz L, Daniel K, Roig I, Bolcun-Filas E, Xu H, Boonsanay V, Eckmann CR, Cooke HJ, Jasin M, Keeney S, et al. (2009) Mouse HORMAD1 and HORMAD2, two conserved meiotic chromosomal proteins, are depleted from synapsed chromosome axes with the help of TRIP13 AAA-ATPase. PLoS Genet 5: e1000702
Pubmed: Author and Title
CrossRef: Author and Title
Google Scholar: Author Only Title Only Author and Title

Yang F, De La Fuente R, Leu NA, Baumann C, McLaughlin KJ, Wang PJ (2006) Mouse SYCP2 is required for synaptonemal complex assembly and chromosomal synapsis during male meiosis. J Cell Biol 173: 497-507
Pubmed: Author and Title
CrossRef: Author and Title
Google Scholar: Author Only Title Only Author and Title

Yuan L, Pelttari J, Brundell E, Björkroth B, Zhao J, Liu JG, Brismar H, Daneholt B, Höög C (1998) The synaptonemal complex protein SCP3 can form multistranded, cross-striated fibers in vivo. J Cell Biol 142: 331-9
Pubmed: Author and Title
CrossRef: Author and Title
Google Scholar: Author Only Title Only Author and Title

Zickler D, Kleckner N (1999) Meiotic chromosomes: integrating structure and function. Annu Rev Genet 33: 603-754
Pubmed: Author and Title
CrossRef: Author and Title
Google Scholar: Author Only Title Only Author and Title